minerals

MDPI

Article

Effects of Size and Mechanical Pre-Treatment on Aluminium Recovery from Municipal Solid Waste Incineration Bottom Ash

Mertol Gökelma [1,*], Utku Hatipoğlu [1], Alicia Vallejo-Olivares [2], Rabia Önen Tüzgel [1], Olcay Kıvrak [1], Elif Bazoğlu [1], Zeynep Su Çizen [1] and Gabriella Tranell [2]

[1] Department of Materials Science and Engineering, Izmir Institute of Technology, 35430 Izmir, Türkiye; utkuhatipoglu@iyte.edu.tr (U.H.); olcaykivrakk@gmail.com (O.K.)
[2] Department of Materials Science and Engineering, Norwegian University of Science and Technology, 7491 Trondheim, Norway; gabriella.tranell@ntnu.no (G.T.)
* Correspondence: mertolgokelma@iyte.edu.tr

Abstract: Municipal solid waste (MSW) is incinerated to reduce the volume and recover energy and materials. The generation of MSW has been increasing over the past few decades due to the increase in population and changing consumption habits. Rising environmental and economic concerns have increased the importance of waste treatment and recovery. Currently, MSW may take three alternate or parallel routes: direct recycling, incineration, or landfill, depending on the country and location. MSW incineration has three products in addition to energy: bottom ash, fly ash, and off-gas. After incineration, bottom ash usually still contains many materials to be recovered, such as glass, ceramics, and metals with a degree of oxidation. This study focuses on aluminium recovery from MSW incineration bottom ash from two different countries. The 2–30 mm fraction of aluminium particles was characterized in terms of its size, shape, and oxide thickness, and its effects on aluminium recovery were investigated. In addition, the ability of mechanical pre-treatment to remove oxides prior to melting was studied. The results were compared with the analytical modeling developed in this study. An increasing particle size and surface area resulted in an increase in aluminium recovery. Mechanical pre-treatment increased the yield for smaller particles to a larger extent than larger particles due to the difference in the oxide/metal ratio.

Keywords: incineration; oxidation; solid waste; recycling; compaction

Citation: Gökelma, M.; Hatipoğlu, U.; Vallejo-Olivares, A.; Önen Tüzgel, R.; Kıvrak, O.; Bazoğlu, E.; Çizen, Z.S.; Tranell, G. Effects of Size and Mechanical Pre-Treatment on Aluminium Recovery from Municipal Solid Waste Incineration Bottom Ash. *Minerals* **2024**, *14*, 1006. https://doi.org/10.3390/min14101006

Academic Editor: Hugo Marcelo Veit

Received: 3 September 2024
Revised: 29 September 2024
Accepted: 3 October 2024
Published: 5 October 2024

1. Introduction

The increasing population and changing consumption habits have resulted in a growing volume of municipal solid waste (MSW). The amount of MSW generated in the world annually is estimated to be 3.4 billion tonnes by 2050 [1]. MSW contains metal, ceramic, glass, plastic, and organic fractions. The widespread utilization of incineration applications for MSW in the solid waste management industry ensures an up to 90% reduction in volume and at least 70% reduction in mass compared to initial values due to the burning of organics [2].

End-of-life products are recycled, landfilled, and/or incinerated to various extents, depending on the country. Globally, around 19% of waste generated is recycled, and 11% is incinerated [3]. Direct recycling is the most effective process for material recovery. However, social behavior and governmental regulations directly affect the amount and type of metals being recycled. Metallic fractions oxidize and are contaminated by the surrounding materials, which reduces the recoverable amount of the metal. The rest of the waste is landfilled, which is the worst scenario for the environment due to soil acidification and contamination as well as the economic impact.

Figure 1 presents the recycling and incineration ratios of European countries in 2021. It can be observed that Norway, Finland, and Sweden incinerate more than 50% of their MSW.

On the other hand, Switzerland, Belgium, Luxembourg, Denmark, the Netherlands, Austria, Germany, Slovenia, and Italy recycle more than 50% of their MSW. These two groups of countries landfill less than 10% (except Italy ≈19%) of their total MSW. From the 32 countries given in Figure 1, 9 countries (Cyprus, Greece, Malta, Romania, Montenegro, North Macedonia, Albania, Türkiye, and Kosovo) landfill more than 70% of their MSW which corresponds to approximately 40 million tons of MSW landfilled.

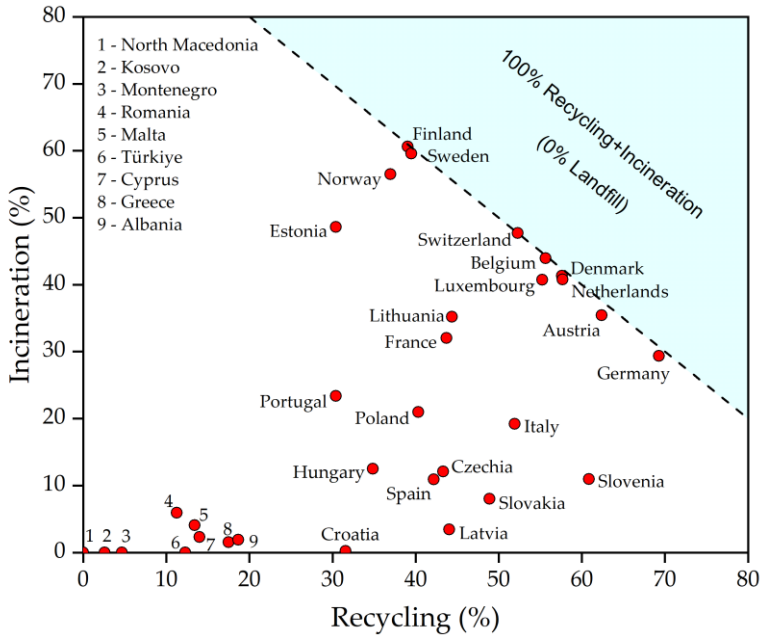

Figure 1. Incineration and recycling ratios of MSW in 2021 (data: Eurostat) [4].

Figure 2 presents the annual municipal waste generation per country as a function of their gross domestic product (GDP). Although a linear correlation cannot be seen, it can be stated that countries generate more waste with increasing GDP. Only Sweden and the Netherlands are among the countries with a higher GDP than the EU (European Union) and generate less waste than the EU on average.

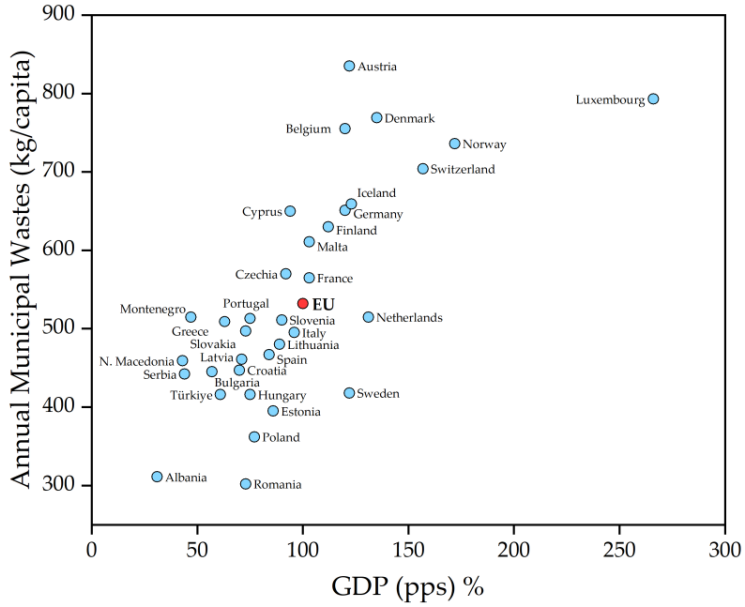

Figure 2. Annual MSW production per capita in comparison with the GDP of different European countries in 2021 (Data: Eurostat) [4].

Municipal solid waste incineration (MSWI) can be converted using three different types of combustion devices: rotary furnaces, fluidized beds, and grate incinerators. European MSWI is predominantly performed in grate-firing-type incinerators. The waste is introduced into the furnace and is carried by the moving grate through the incineration zone and discharged after the incineration is completed. The average temperature on the bed surface is approximately 900 °C; however, the temperature distribution in such furnaces is heterogeneous [5]. Bunge reported that 80% of materials during incineration are subjected to temperatures between 700 °C and 1100 °C [6].

The outputs of a MSW incineration process are heat, off-gas, bottom ash, and fly ash [7]. Both ashes represent the unburned fractions of the waste. Fly ash is mainly fine oxidic particles collected on the way to the chimney [8]. Bottom ash consists of larger particles, including ceramic, glass, and metals [9]. The bottom ash is sorted by the type of materials, such as glass, ceramic, aluminium, iron, and copper [10]. In addition, due to the wide range of particle size, the ash is also sorted according to size. While the size fraction below 2 mm can be used in construction materials, fractions over 2 mm contain a significant number of metals to be recovered [11].

Warrings and Fellner reported that approximately 11 wt.% of the aluminium is lost due to oxidation in incineration plants [12]. Chen et al. [13] investigated the metallic aluminium content of the aluminium fraction in bottom ash for sizes between 0.5 and 1.6 mm, and an aluminium content of 6 to 71 wt.% was reported. Gökelma et al. reported that the oxide thickness of the aluminium fraction in bottom ash was 68 µm on average, but no correlation was found between the oxide thickness and particle size or origin [14]. Vallejo Olivares et al. reported a life cycle assessment of the recycling of waste streams, including bottom ash in rotary furnaces. The study concluded that recycling 1 tonne of waste streams with a metal yield of 72% saves 13.2 t CO_2 eq [15]. Syvertsen et al. studied the yield and composition of aluminium bottom ash particle ranging from 5 to 50 mm (mostly in the range of 5–25 mm). Heavy elements such as Pb, Hg, Bi, Cd, and Sb were detected from one to several hundred ppm, and a 90% to 96% metal yield was reported [16]. Marthinsen et al. assessed the possibility of AlSi10Mg alloy production from bottom ash. Salt treatment and arc remelting were both applied, and with Si and Mg additions the AlSi10Mg alloy was obtained. Studies regarding economic feasibility and impurity issues are still ongoing [17]. MSW and its fractions in bottom ash are very heterogeneous in terms of composition and size, which makes characterization very difficult and limits the modeling of expected efficiencies. Therefore, more measurements and characterization studies are needed to better understand the recyclability of these types of materials.

This study investigates the effects of size, shape, and the mechanical pre-treatment of the MSWI aluminium fraction on the formed oxide thickness during the incineration procedure and metal yield. Aluminium fractions from two countries (the United Kingdom and the United States of America) were remelted before and after compaction as a form of pre-treatment to assess the metal yield. The samples were analyzed under computed tomography (CT) analysis and Scanning Electron Microscope (SEM), and their oxide thicknesses were measured using ImageJ (version 1.54g) software. EDS and XRF analysis were performed to measure the composition of the oxide layer. An analytical model was developed to approximate the metal yield results, and a model was proposed that is independent of the bottom ash source. Predicted aluminium yield values for particles that are 1 to 30 mm with an oxide layer of up to 500 µm are shown.

2. Materials and Methods

2.1. Materials

The bottom ash samples used in this study were received from a European recycling company. Samples were collected from incinerators in the USA and the UK and dry-sorted. Industrial sorting was achieved in three size groups, which were 2–6, 6–12, and 12–30 mm. However, due to industrial sorting techniques and the heterogeneity of the material, further separation of glass, dust, ferrous, and non-ferrous fractions in the bottom

ash was performed manually as part of the current study. Compaction was applied for some bottom ash samples under 100 kN for 5 s to observe the effects of compaction.

2.2. Remelting

The sample size groups from different sources were remelted in a laboratory-scale resistance chamber furnace at 800 °C. In addition, 2–6 and 6–12 mm fractions were compacted into cylindrical briquettes using uniaxial pressure to see the effect of compaction on the metal yield. A clay-bonded graphite crucible with a volume of 0.3 lt was used for remelting. The remelting was carried out under a salt flux to remove the thick oxide layer and prevent further metal losses during melting. The salt flux consisted of chlorides NaCl-KCl (70:30 wt.%) and 2 wt.% CaF_2 was added to promote coagulation. After melting, the melt in the crucible was stirred with a graphite rod and the crucible was allowed to cool in the furnace. After cooling to room temperature, the salt dross was washed out, and the metal fraction was collected.

2.3. Characterization

The samples in all size ranges were analyzed using the image analysis program ImageJ to calculate their 2D surface area, perimeter, and circularity. Three samples were randomly selected from each size range and origin and mounted in epoxy. After sanding and polishing, the cross-section of samples was analyzed under SEM, and oxide layer thicknesses were measured from at least 40 positions from each sample. EDS and XRF analysis were used to assess the composition of the oxide layer of the samples. In addition, compacted bottom ash samples were analyzed using CT to observe the compaction degree and internal porosity.

2.4. Analytical Modeling

An analytical model was developed, which is valid for a broad size range of particles and oxide layers. This model covers most of the oxide/metal ratios possible during incineration. The results were obtained by calculating the oxide mass of bottom ash samples by changing the diameter of the sample and the thickness of the oxide. Particles as shown in Figure 3 with a radius of "r" with an oxide thickness of "x" were used for the model, where r ranges from 1 to 30 mm and x is 10 to 500 µm. The assumptions made for the model are shown below:

- Bottom ash particles are spherical;
- Oxide and metal phases have the same porosity value;
- Oxide thickness is the same throughout the entire surface;
- The density of the metal alloy is 2.7 g/cm^3;
- The density of the oxide layer is 3.99 g/cm^3.

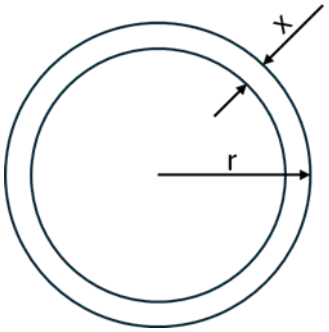

Figure 3. Schematic of a spherical bottom ash particle with an oxide layer.

The mass of the outer oxide layer and the metal core were calculated by multiplying the volume and density of each. The metal yield was calculated by the ratio of metal to the entire sample, as shown in Equation (1). ρ_{Al} is the density of aluminium, ρ_{oxide} is the

density of the oxide layer, π is the number of pi, r is the radius of the sample, and x is the thickness of the oxide layer.

$$\text{Predicted Metal Yield} = \frac{\rho_{Al} \cdot {}^{4}/_{3}\pi(r-x)^{3}}{\rho_{Al} \cdot {}^{4}/_{3}\pi(r-x)^{3} + \rho_{oxide} \cdot {}^{4}/_{3}\pi\left(r^{3} - (r-x)^{3}\right)} \quad (1)$$

3. Results and Discussion

The length and surface area of samples from the aluminium fraction were characterized using ImageJ image analysis software, and samples were sorted into four groups for each country. Figure 4 presents the picture of three samples from the USA, which was used for image analysis. The same process was conducted for every particle group, and, in total, 1150 samples were analyzed.

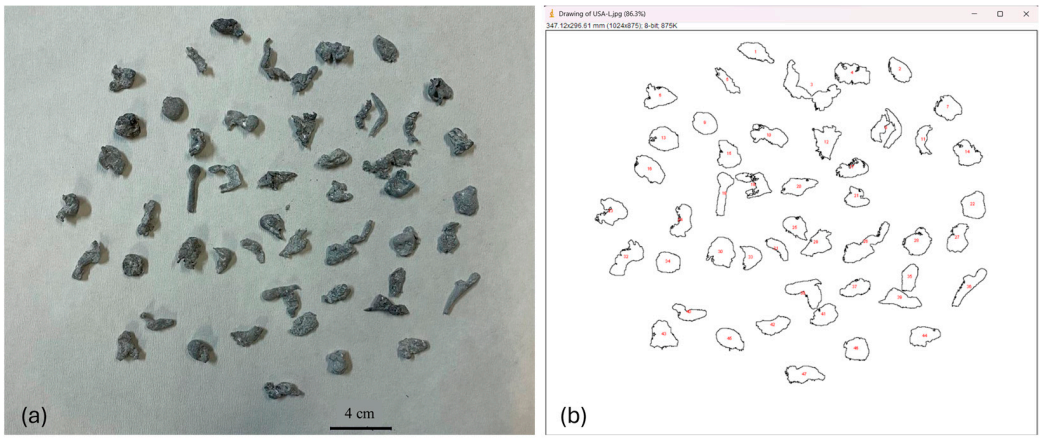

Figure 4. (**a**) A representative picture of the USA 3-sample group; (**b**) image analysis screen shot of the samples.

Figure 5 shows the computed tomography analysis picture of compacted bottom ash samples. It can be observed from the picture that the direct contact of samples was achieved. Also, glass contamination could be observed in the structure, which is common due to the inefficient sorting of fractions. The internal porosity was measured as 22%, which is acceptable due to the high content of hard oxides on the surface. Due to the high hardness of oxides, cracked oxides were observed in powder form during compaction. In total, 1.4 ± 0.4 wt.% weight loss was observed in 18 compaction tests. The collected powder was analyzed by XRF. XRF results showed that the powder consisted of 31% Al_2O_3, 27% SiO_2, 16% CaO, 3% Fe_2O_3, and 3% Na_2O (in wt.%), which are typical oxides found on aluminium scraps and incinerated waste.

Table 1 shows the length and surface area of the samples as well as their metal yield values after remelting under salt flux. The length was measured by taking the longest axis of the sample, which is an area that represents the two-dimensional area of the samples, as seen in Figure 4b. The aluminium yield after remelting the bottom ash samples was calculated using Equation (2).

$$\text{Metal Yield} = \frac{m_{\text{recovered Al}}}{m_{\text{input Al-fraction}}} \times 100\% \quad (2)$$

where $m_{\text{input Al-fraction}}$ is the total mass of charged bottom ash samples and $m_{\text{recovered Al}}$ is the mass of all aluminium droplets recovered via salt remelting. The metal yield was found to be between 71.9 and 95.7 wt.% depending on the size, which is in line with previous studies, which showed yields of 76–93 [14] and 83–92 wt.% [18].

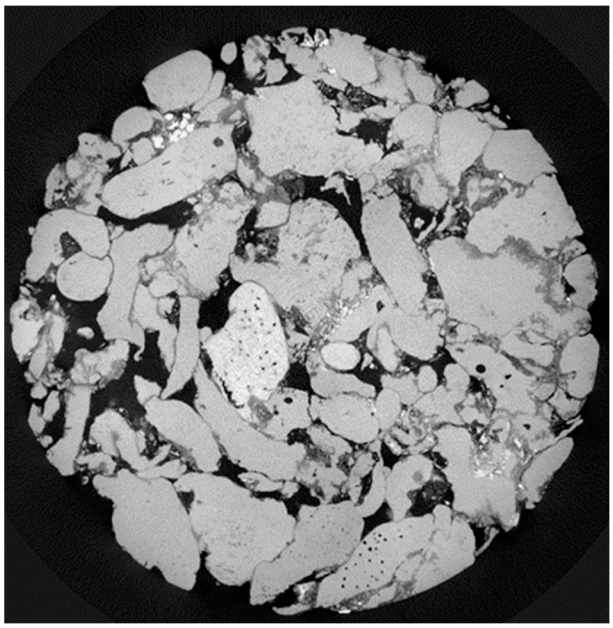

Figure 5. CT analysis of bottom ash samples compacted by uniaxial pressure.

Table 1. Maximum length and surface area measurements of aluminium fraction samples.

	Av. Axis Length (mm)	Std of Length (%)	Av. 2D Area (mm^2)	Std of Area (%)	Al Yield (%)	Al Yield after Compaction (%)
USA 1	5	2.82	77	58.31	71.91	77.6
UK 1	5.6	2.29	76	62.37	77.15	80.1
USA 2	8.6	2.57	164	43.60	81.30	83.8
UK 2	9.3	2.66	155	44.32	82.96	83.2
USA 3	14.3	1.68	277	32.56	86.59	-
UK 3	15.9	1.55	217	26.04	83.53	-
USA 4	27.9	2.93	357	35.57	95.67	-
UK 4	28	2.76	353	29.18	91.84	-

Figure 6 shows the metal yield of the four fractions from the two countries shown in Table 1 as a function of size. Each particle was measured as mentioned above, and the average of their longest length (with a standard deviation of 1.55% to 2.93%) used is shown in Figure 6. A clear trend can be observed with an R^2 value of 0.88, which indicated that increasing the size of the aluminium fraction in bottom ash results in a higher metal yield. An almost 25% yield difference was observed between a 5 and 28 mm particle length. For the mentioned size range, a linear yield difference is expressed, as shown below:

$$\text{Metal yield} = 0.0775\text{L} + 0.7278 \quad (3)$$

where, metal yield is calculated via Equation (2) and L is the max length of the sample calculated via ImageJ.

Further investigation was conducted to determine the effect of surface area on the metal yield. Figure 7 shows an increase in metal yield with an increase in surface area similar to the trend seen between metal yield and length; however, a deviation in surface area measurements was observed between 26% and 62% due to for the irregular shape of the bottom ash particles. Due to high deviation in surface area measurements, it is recommended to use the length instead of the area to define the relation. The linear trend with an R^2 value of 0.8668 can be expressed as follows:

$$\text{Metal yield} = 0.0635\text{L} + 0.7058 \quad (4)$$

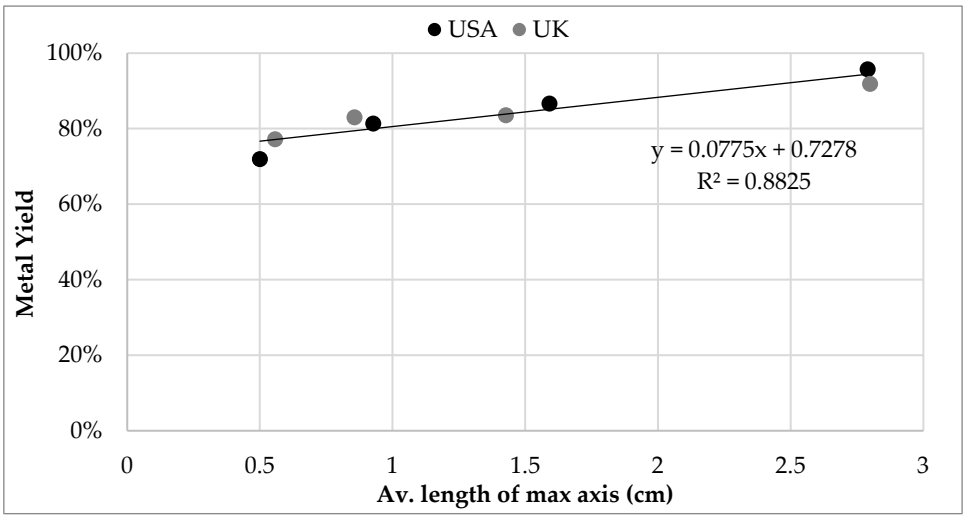

Figure 6. Metal yield of each size fraction as a function of the average max axis of samples.

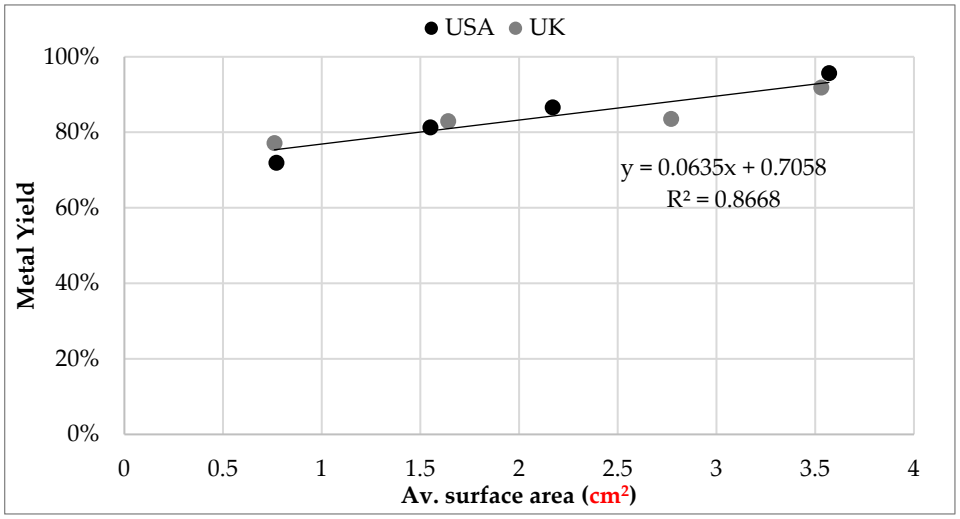

Figure 7. Metal yield of each size fraction as a function of the average surface area of samples.

Figure 8 presents each oxide thickness measurement under SEM for bottom ash samples from UK and USA. Multiple SEM pictures were taken from each sample, and random locations were measured.

Table 2 summarizes the 906 measurements performed using ImageJ in terms of the oxide thickness fractions. The thickness results were grouped as <40, <50, 50–100, and >100 µm. In total, 63.5% of all measurements were below 50 µm, 25.9% were between 50 and 100 µm, and 10.6% were thicker than 100 µm. The mean thickness value of all 906 measurements was 70 µm. A significant difference between UK and USA samples were not observed in terms of oxide thickness distribution.

Table 2. Oxide thickness distribution in all samples.

Oxide Thickness (µm)	UK (% of Samples)	USA (% of Samples)	Average, All Samples (%)
<40	53.6	51.9	52.1
<50	64.6	62.3	63.5
50–100	23.4	28.7	25.9
>100	12.0	9.0	10.6

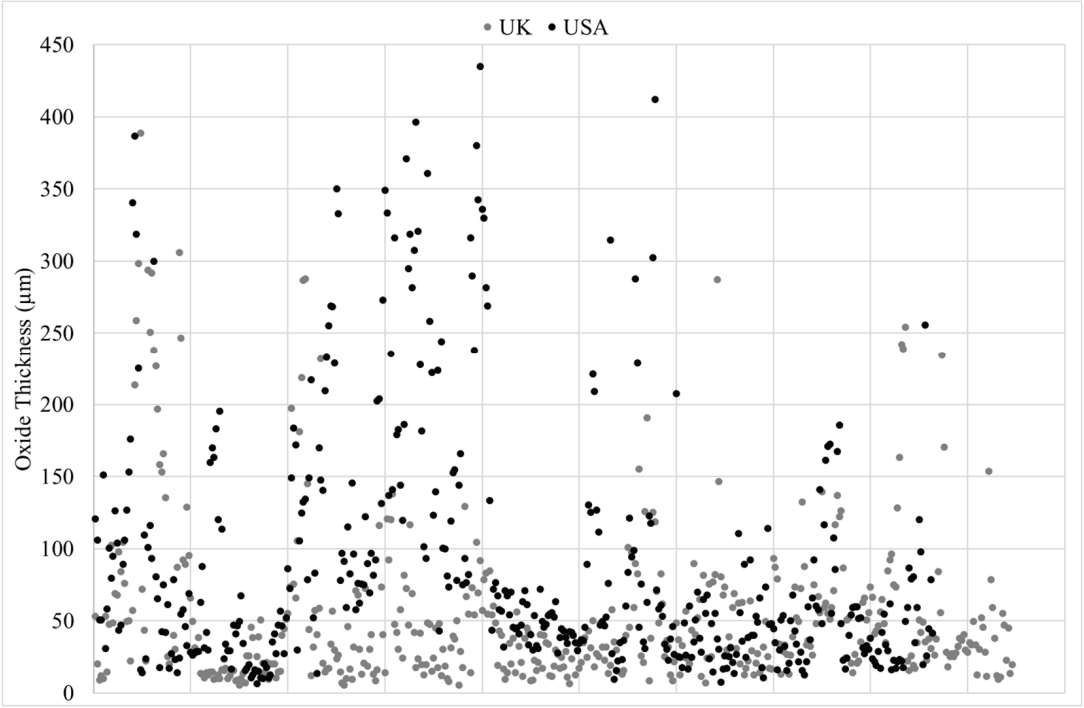

Figure 8. Oxide thickness measurement for 906 measurement points of samples from the UK and USA.

Figure 9 shows a typical cross-section of an aluminium sample in bottom ash. The oxide layer can be clearly seen in a darker color. The layer is not homogeneous, and the thickness varies throughout the surface.

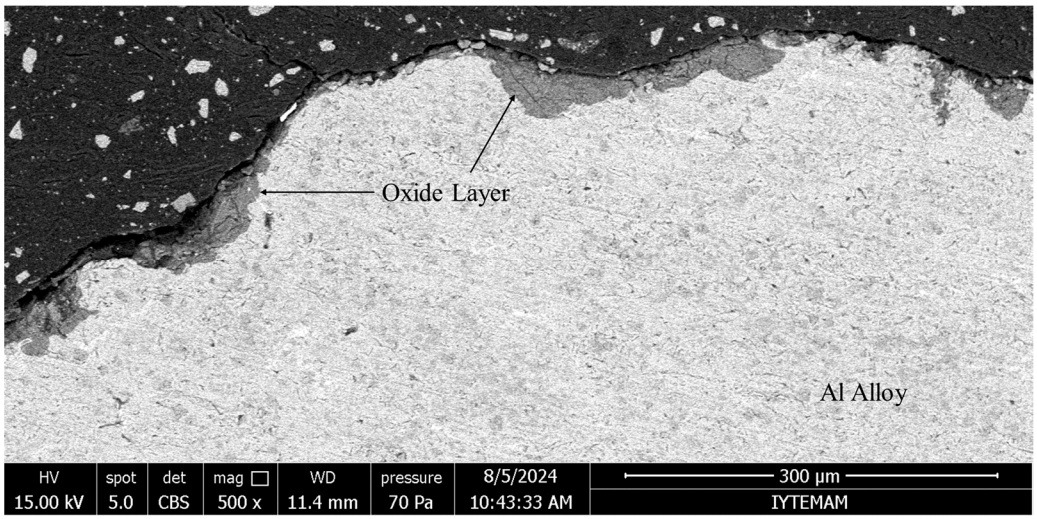

Figure 9. SEM image of the cross-section of a representative bottom ash sample.

The oxide layer of the samples was analyzed by EDS. A high oxygen and aluminium content were observed in all samples, as expected, due to the heavy oxidation of aluminium during incineration. Na, K, and Cl were found in all samples. Cl content mainly originates from PVC, food waste, and batteries [19]. This can lead to HCl formation during the remelting of the aluminium fraction, and thermal decomposition up to 600 °C can lead to molecular Cl_2 [20]. In addition, bottom ash materials, especially fine fractions, can be used in secondary building materials, but the Cl content becomes a challenge due to strict regulations for building materials [21]. Chloride content can be found at up to 5 wt.% depending on the fraction and size of the sample [22]. Sulphur content in the samples can

also lead to the formation of harmful gasses, which should be taken into account during recycling/remelting processes.

Analytical Modeling

Figure 10 presents the modeling results for bottom ash particles from 1 to 30 mm in diameter with an oxide layer of up to 500 µm. Increasing the sample size and decreasing oxide thickness increases the metal yield due to the decreasing oxide/metal mass ratio. The predicted yields for 70 µm (mean value of measured samples) oxide thickness are 55% for 1 mm, 74% for 2 mm, 89% for 5 mm, 94% for 10 mm, 97% for 20 mm, and 98% for 30 mm aluminium samples. The degree of oxidation becomes more important with the decreasing sample size and effects the metal yield significantly.

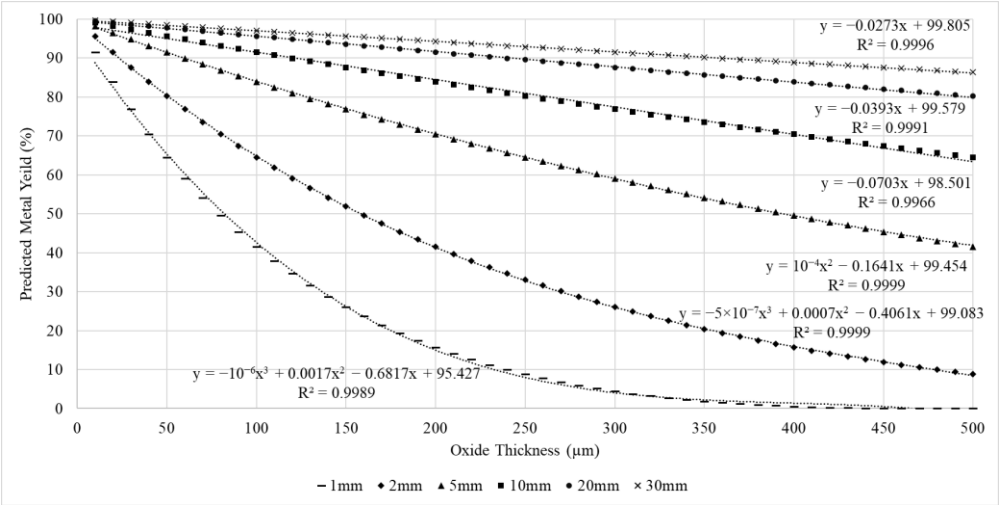

Figure 10. Metal yield predictions of changing particle size and oxide thickness.

In order to compare the modeling results with experimental results, calculations were also conducted for the average particle sizes used in the remelting experiments. Table 3 presents the modelling results where x is oxide thickness (mm) and y represents the predicted metal losses.

Table 3. Trendlines calculated by the analytical model for the average particle sizes used in remelting experiments.

Average Particle Size (mm)	Formula	R^2	Equation
9	$y = -2 \times 10^{-8} \times 3 + 5 \times 10^{-5}x^2 - 0.0982x + 99.992$	1	(5)
15	$y = -0.0505x + 99.281$	0.9984	(6)
28	$y = -0.029x + 99.778$	0.9995	(7)

Figure 11 shows the metal yield results calculated by the model for particles with a homogenous oxide thickness of 70 µm and the results from the remelting experiments. The predicted yield is higher than the experimental results for all sizes. The main reason for this difference is the effect of particle shape. Particles are assumed to be spherical in the modeling, and a spherical shape has a lower specific surface area than the real shape of bottom ash particles. The lower specific surface area results in a lower mass of oxides in comparison with the metal. However, the difference between the model and experiments decreases with increasing particle sizes. This is due to the decreasing oxide/metal mass ratio with increasing particle size. It can also be observed that the yield after compaction increases up to 5% due to the loss of the oxide layer during compaction. Compaction works like mechanical pre-treatment, decreasing the non-metal content. However, this

effect decreases with increasing size due to the decreasing oxide/metal ratio. The rafination of the recovered aluminium alloy melt must be improved in further studies since the composition of the recovered alloy may change depending on the season, location, and treatment. The mechanical pre-treatment of bottom ash must be further studied to increase the yield and decrease the usage of salt flux for more sustainable recycling processes.

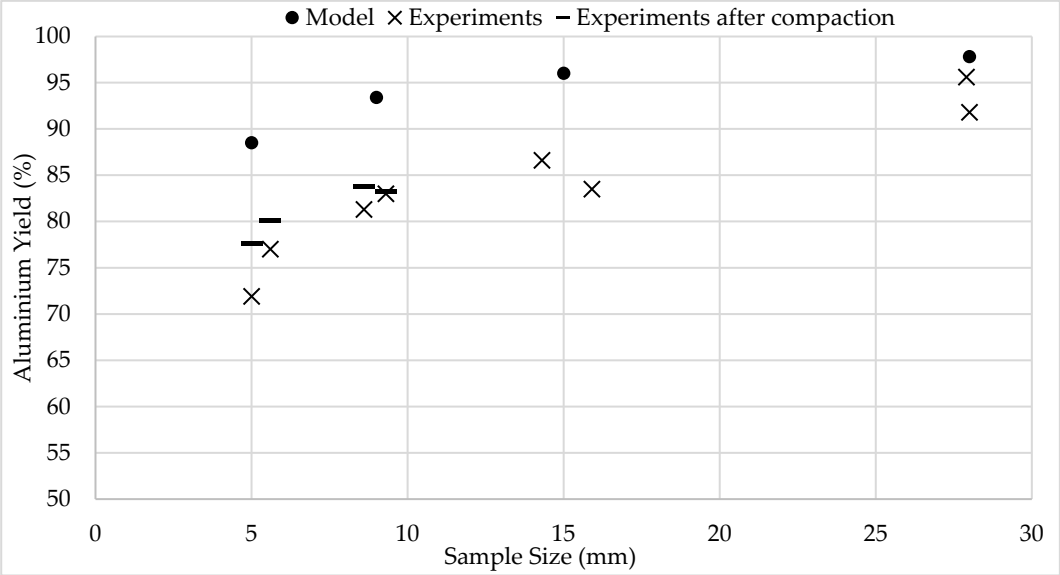

Figure 11. Comparison of the metal yield results calculated by the analytical model and measured by experiments.

4. Conclusions

The effect of particle size, shape, and mechanical pre-treatment has been experimentally studied, and an analytical model has been developed. The following conclusions can be drawn as a result of the research:

- The particle length and surface area have a linear correlation with recoverable aluminium content for bottom ash particles between a 2 and 30 mm fraction.
- Mechanical pre-treatment decreased the oxide content by cracking the oxides, which increased the aluminium yield. However, this effect became less significant with increasing particle size due to a decrease in oxide/metal ratio.
- The analytical model showed a 5% to 15% higher yield for particles with an average size of 28 to 5 mm, respectively. The difference between the model and experiments originated due to the specific surface area difference in spherical to irregular particles.

Author Contributions: M.G.: conceptualization, data curation, formal analysis, methodology, project management, validation, and writing—original draft; M.G. and G.T.: conceptualization, methodology, supervision, validation, and writing—review and editing; A.V.-O. and U.H.: data curation, investigation, methodology, visualization, and writing—review and editing; R.Ö.T., O.K., E.B. and Z.S.Ç.: investigation, methodology, and validation. All authors have read and agreed to the published version of the manuscript.

Funding: This research received no external funding.

Data Availability Statement: The data are contained within the article.

Acknowledgments: The Center for Materials Research at İzmir Institute of Technology is gratefully acknowledged for the sample analyses. The Environmental Research Center at İzmir Institute of Technology is gratefully acknowledged for metal analyses.

Conflicts of Interest: The authors declare there are no conflicts of interests.

References

1. Kaza, S.; Yao, L.; Bhada-Tata, P.; Van Woerden, F. *What a Waste 2.0: A Global Snapshot of Solid Waste Management to 2050*; World Bank Publications: Washington, DC, USA, 2018.
2. Kumar, S.; Singh, D. Municipal solid waste incineration bottom ash: A competent raw material with new possibilities. *Innov. Infrastruct. Solut.* **2021**, *6*, 201. [CrossRef]
3. Joseph, A.M.; Snellings, R.; Nielsen, P.; Matthys, S.; De Belie, N. Pre-treatment and utilisation of municipal solid waste incineration bottom ashes towards a circular economy. *Constr. Build. Mater.* **2020**, *260*, 120485. [CrossRef]
4. Eurostat. Municipal Waste by Waste Management Operations. Available online: https://ec.europa.eu/eurostat/databrowser/view/env_wasmun/default/table?lang=en (accessed on 16 August 2024).
5. Leckner, B.; Lind, F. Combustion of municipal solid waste in fluidized bed or on grate—A comparison. *Waste Manag.* **2020**, *109*, 94–108. [CrossRef] [PubMed]
6. Bunge, R. Recovery of Metals from Waste Incinerator Bottom Ash. 2016. Available online: www.vbsa.ch (accessed on 4 October 2024).
7. Chimenos, J.M.; Segarra, M.; Fernandez, M.A.; Espiell, F. Characterization of the bottom ash in municipal solid waste incinerator. *J. Hazard. Mater. A* **1999**, *64*, 211–222. [CrossRef]
8. Wu, H.Y.; Ting, Y.P. Metal extraction from municipal solid waste (MSW) incinerator fly ash—Chemical leaching and fungal bioleaching. *Enzyme Microb. Technol.* **2006**, *38*, 839–847. [CrossRef]
9. Stabile, P.; Bello, M.; Petrelli, M.; Paris, E.; Carroll, M.R. Vitrification treatment of municipal solid waste bottom ash. *Waste Manag.* **2019**, *95*, 250–258. [CrossRef] [PubMed]
10. Verbinnen, B.; Billen, P.; Van Caneghem, J.; Vandecasteele, C. Recycling of MSWI Bottom Ash: A Review of Chemical Barriers, Engineering Applications and Treatment Technologies. *Waste Biomass Valorization* **2017**, *8*, 1453–1466. [CrossRef]
11. Muchová, L. Wet Physical Separation of MSWI Bottom Ash. Ph.D. Thesis, TU Delft, Delft, The Netherlands, 2010.
12. Warrings, R.; Fellner, J. Current status of circularity for aluminum from household waste in Austria. *Waste Manag.* **2018**, *76*, 217–224. [CrossRef] [PubMed]
13. Chen, B.; Chen, J.; de Mendonça Filho, F.F.; Sun, Y.; van Zijl, M.B.; Copuroglu, O.; Ye, G. Characterization and mechanical removal of metallic aluminum (Al) embedded in weathered municipal solid waste incineration (MSWI) bottom ash for application as supplementary cementitious material. *Waste Manag.* **2024**, *176*, 128–139. [CrossRef] [PubMed]
14. Gökelma, M.; Vallejo-Olivares, A.; Tranell, G. Characteristic properties and recyclability of the aluminium fraction of MSWI bottom ash. *Waste Manag.* **2021**, *130*, 65–73. [CrossRef] [PubMed]
15. Olivares, A.V.; Pastor-Vallés, E.; Pettersen, J.B.; Tranell, G. LCA of recycling aluminium incineration bottom ash, dross and shavings in a rotary furnace and environmental benefits of salt-slag valorisation. *Waste Manag.* **2024**, *182*, 11–20. [CrossRef] [PubMed]
16. Syvertsen, M.; Ludwig, T.; Rist, S.; Ellingsen, K. Use of Incinerator Bottom Ash (IBA) in Aluminium Recycling. In *Light Metals 2022*; Eskin, D., Ed.; Springer International Publishing: Cham, Switzerland, 2022; pp. 1051–1055.
17. Marthinsen, A.; Graff, J.S.; Syvertsen, M.; Ellingsen, K.; M'Hamdi, M. Towards Formulation of AlSi10Mg Alloy from Incinerator Bottom Ash. In *Light Metals 2022*; Eskin, D., Ed.; Springer International Publishing: Cham, Switzerland, 2022; pp. 1056–1065.
18. Gökelma, M.; Meling, I.; Soylu, E.; Kvithyld, A.; Tranell, G. A method for assessment of recyclability of aluminum from incinerated household waste. In *Light Metals 2019*; Minerals, Metals and Materials Series; Springer International Publishing: Cham, Switzerland, 2019; pp. 1359–1365. [CrossRef]
19. Ma, W.; Wenga, T.; Frandsen, F.J.; Yan, B.; Chen, G. The Fate of Chlorine during MSW Incineration: Vaporization, Transformation, Deposition, Corrosion and Remedies. *Prog. Energy Combust. Sci.* **2020**, *76*, 100789. [CrossRef]
20. Frandsen, F.J.; Frandsen, F.J.; van Lith, S.C.; Korbee, R.; Yrjas, P.; Backman, R.; Obernberger, I.; Brunner, T.; Jöller, M. Quantification of the release of inorganic elements from biofuels. *Fuel Process. Technol.* **2007**, *88*, 1118–1128. [CrossRef]
21. Chandler, A.J.; Eighmy, T.T.; Hjelmar, O.; Kosson, D.S.; Sawell, S.E.; Vehlow, J.; van der Sloot, H.A.; Hartlén, J. *Municipal Solid Waste Incinerator Residues*; Elsevier: Amsterdam, The Netherlands, 1997.
22. Yang, S.; Saffarzadeh, A.; Shimaoka, T.; Kawano, T. Existence of Cl in municipal solid waste incineration bottom ash and dechlorination effect of thermal treatment. *J. Hazard. Mater.* **2014**, *267*, 214–220. [CrossRef] [PubMed]